An Iterative Dual Reciprocity Method for a Class of Infiltration Problems in Two-Layered Soils with Different Types of Root-Water Uptake

Imam Solekhudin, Anny Kartika Sari, and Faizal Makhrus

Abstract—This study delves into the investigation of steady infiltration problems within a two-layered soil, featuring periodic channels, and taking into account the presence of root-water uptake, with four different types of root-water uptake considered. The problems are governed by a set of Richards' equations accompanied by boundary interface conditions. To tackle these problems, we transform the system of Richards' equations, along with the corresponding boundary conditions, into a set of steady diffusion-convection equations with transformed boundary conditions. This mathematical model is then addressed using a numerical approach that leverages the Iterative Dual Reciprocity Method (IDRM). Through this numerical method, we obtain solutions that characterize the distribution of hydraulic conductivity within the soil and root-water uptake in the root zone. Furthermore, we conduct comparisons and analyze the root-water uptake resulting from the four different types of root-water uptake. The findings of this study provide insights into how the type of root influences the amount of water absorbed by the roots.

Index Terms—Steady infiltration, two-layered soil, iterative dual reciprocity method, root-water uptake functions.

I. INTRODUCTION

Numerous researchers have conducted investigations related to water infiltration. Among them are Batu [6], Gardner [16], Lobo et al. [24], Mandal and Waechter [27], Philip [32], Solekhudin and Ang [39], and Solekhudin [42], [43]. These researchers primarily focused on problems related to steady infiltration. Batu [6] examined the phenomenon of steady infiltration originating from both single and periodic strip sources. Gardner [16] delved into the study of water flow in unsaturated soil, particularly focusing on situations involving evaporation from a water table.. Lobo et al. [24] undertook research on water infiltration in unsaturated soil containing impermeable materials. Mandal and Waechter [27] explored water infiltration emanating from a buried circular cylinder. Philip [32] investigated water infiltration from buried point and circular cavities. Solekhudin and

Imam Solekhudin is a Professor at Department of Mathematics, Faculty of Mathematics and Natural Sciences, Universitas Gadjah Mada, Yogyakarta, 55281 Indonesia. (corresponding author, phone: 62-274-552243; e-mail: imams@ugm.ac.id.)

Anny Kartika Sari is an Associate Professor at Department of Computer Science and Electronics, Faculty of Mathematics and Natural Sciences, Universitas Gadjah Mada, Yogyakarta, 55281 Indonesia. (e-mail: a_kartikasari@ugm.ac.id.)

Faizal Makhrus is an Assistant Professor at Department of Computer Science and Electronics, Faculty of Mathematics and Natural Sciences, Universitas Gadjah Mada, Yogyakarta, 55281 Indonesia. (e-mail: faizal_makhrus@ugm.ac.id.)

Ang [39] idelved into the examination of water infiltration originating from periodic channels while considering root-water uptake. Continuing from their earlier work, Solekhudin [43] expanded the study in [39] by incorporating various types of root-water uptakes.

In contrast, time-dependent infiltration issues have been explored by researchers such as Clements and Lobo [12], Lomen and Warrick [26], Solekhudin and Ang [40], [41], and Warrick and Lomen [50]. Clements and Lobo [12] investigated water infiltration from irrigation channels using a boundary element method. Lomen and Warrick [26] conducted research on water infiltration from line sources. Solekhudin and Ang [40] explored water infiltration from periodic trapezoidal channels. Building on their previous work, Solekhudin and Ang [41] expanded their study in [40] by incorporating considerations for root-water uptake. Warrick and Lomen [50] focused on the study of infiltration from strip and disc sources.

An essential focus of research within the field of water infiltration pertains to the process when it occurs in layered soils. The study of water infiltration in layered soils represents a fundamental component of soil physics. This line of research can be traced back to its origins in studies conducted in rice fields, where a distinctive configuration was employed, maintaining a saturated zone above an unsaturated zone, with fine soil positioned over coarse soil [46]. These investigations have taken various forms, encompassing analytical studies [47], [3], [25], numerical simulations [29], [38], [44], [45], and experimental research [53].

Srivastava and Yeh conducted analytical investigations into transient infiltration problems, with a specific focus on scenarios involving the water table. Their research encompassed both homogeneous and layered soils [47]. However, their proposed method may not be suitable for addressing infiltration issues in layered soils characterized by varying soil coarseness. In response to this limitation, Barontini et al. introduced an analytical method designed to handle infiltration problems where hydraulic conductivity decreases exponentially with depth [3]. Nevertheless, the approach presented by Barontini and colleagues may not be applicable when the hydraulic conductivity in the lower layer exceeds that in the upper layer. To address this challenge, De Luca and Cepeda proposed an analytical approach capable of addressing one-dimensional infiltration into two-layered soils of any composition [25].

In addition to analytical approaches, finite difference methods (FDM) have been utilized to investigate one-dimensional flow in layered soils. Ross and Bristow, for instance, employed FDM for simulating one-dimensional water move-

ment in layered soils [38]. Oldenburg and Pruess worked on the study of a capillary barrier that forms at the interface of a fine soil layer overlying a coarse soil layer using FDM [29]. Havercamp and Vauclin estimated finite difference interblock hydraulic conductivity values for transient unsaturated flow problems [17]. Solekhudin [45] utilized a dual reciprocity method to tackle the issue of infiltration from periodic trapezoidal channels into two-layered soils characterized by different types of soils, including variations in soil types.

In the investigation of problems related to infiltration in two-layered soils, researchers have extensively employed numerical techniques to solve the Richards equation, with a notable focus on the application of finite element methods (FEM). This approach has been used in various studies, as evidenced by references such as [7], [8], [10], [20], [21], [22], [30], [48].

Belfort and Lehmann employed FEM to compare one-dimensional unsaturated flow scenarios using equivalent conductivities [7]. Brunone et al. explored one-dimensional infiltration into layered soils, considering different estimates of the interlayer conductivity [8]. Celia et al. developed a comprehensive numerical solution for mass-conservative unsaturated flow [10]. Li et al. utilized a local discontinuous Galerkin approximation to solve the Richards equation [20]. Building upon the earlier work in [20], Li et al. extended their research by employing an adaptive local discontinuous Galerkin approximation to address the Richards equation [21]. Lima-Vivancos and Voller used FEM to solve a problem involving saturated flow variability in layered media [22]. Pall et al. examined the transient movement of soil moisture through layered soil [30]. In a separate study, van Dam and Feddes investigated issues related to infiltration, evaporation, and shallow groundwater levels [48].

While the finite element method (FEM) has been widely utilized, it is not without its shortcomings. One notable limitation is the discontinuity of normal flux across element interfaces, leading to a lack of mass conservation within elements, as documented in references such as [13], [14], [28].

To address this issue, two numerical methods that have garnered significant attention among scientists and engineers are the boundary element method (BEM) and the dual reciprocity method (DRM). These methods offer distinct advantages over finite element methods (FEM) and finite difference methods (FDM). In addition to addressing the limitations of FEM mentioned earlier, one of the significant advantages offered by the boundary element method (BEM) and the dual reciprocity method (DRM) is the reduction of the problem dimension by one and the capability to assess solutions at any point within the problem domain, as demonstrated in references such as [18], [55].

Researchers have effectively used both the Boundary Element Method (BEM) and the Dual Reciprocity Method (DRM) to tackle infiltration problems in homogeneous soils, as evidenced by the studies conducted by researchers such as [12], [39], [40], [41], [43]. To employ BEM, it is essential to derive the fundamental solution of the governing equation tailored to the specific problem being investigated. In the context of infiltration problems, this involves obtaining the fundamental solution for either the Helmholtz equation or the diffusion-convection equation.

In contrast, the Dual Reciprocity Method (DRM) does not necessitate intricate fundamental solutions. It relies on a more straightforward fundamental solution, often that of Laplace's equation. Furthermore, DRM is versatile and capable of solving infiltration problems, even when root-water uptake is a factor, whereas BEM may not be well-suited for such situations. This underscores the flexibility of DRM in comparison to BEM as a numerical method for addressing a diverse array of infiltration problems.

The majority of previous research on water flow through layered soils has predominantly centered on one-dimensional problems. Consequently, the aim of this study is to establish a mathematical model for simulating two-dimensional water infiltration scenarios within two-layered soils while considering the influence of root-water uptake. This investigation extends and expands upon the findings previously presented in a prior study [45].

In this research, we have utilized an Iterative Dual Reciprocity Method (IDRM) to address the formulated model. By employing this method, we are able to transform the model into a one-dimensional problem, simplifying the computational process. Dealing with the nonlinearity of the boundary conditions at the interface requires the implementation of iterative steps within the IDRM framework. Our application of the IDRM is specifically geared towards solving water infiltration problems originating from periodic trapezoidal channels into two-layered soils that encompass various types of root-water uptake. The primary objective is to investigate the influence of the root's type on water uptake.

II. PROBLEM FORMULATION

In this research, we investigate steady infiltration problems originating from periodic trapezoidal channels within two-layered soils, while considering four different types of root-water uptake. These channels exhibit a surface area of $2L$ per unit length of the channels, with the distance between the centers of adjacent channels is $2(L + D)$. The channels have a width and a depth of $4L/\pi$ and $3L/2\pi$, respectively.

The upper layer contains a root zone, which is characterized by dimensions of $2X_m$ in width and Z_m in depth. These channels maintain a constant water level, and water infiltration rate is assumed to be constant, denoted as v_0. To maintain consistency with prior works [2], [24], [39], we make certain assumptions. We assume that the channels are sufficiently long and numerous and that their geometry remains constant in the direction parallel to their length.

The top layer is characterized by a thickness of D_1, and the lower layer is situated above the water table and extends to a depth of D_2. Consequently, the problems we are addressing can be treated as two-dimensional in nature. Since the problem exhibits symmetry about the center of each channel and any line positioned at a distance of $L + D$ from the channel's center, we can depict the problem's geometric configuration using a Cartesian coordinate system designated as XOZ. This coordinate system is bounded by the lines $X = 0$, $X = L + D$, $Z = 0$, and $Z = D_1 + D_2$. With these assumptions and descriptions, our objective is to investigate how the type of roots influences the amount of water absorbed from the soil.

III. BASIC EQUATIONS

In this section, we will provide a brief overview of the mathematical model and the solution method for the problems described in the previous section. One of the commonly used models to simulate water infiltration in unsaturated soil with root water uptake is the Richards' equation [33], [36], [35], [37], [51], formulated as follows:

$$\frac{\partial \theta}{\partial t} = \nabla . (K \nabla h) - \frac{\partial K}{\partial Z} - S, \tag{1}$$

which can be written as

$$\frac{\partial \theta}{\partial t} = \frac{\partial}{\partial X}\left(K\frac{\partial h}{\partial X}\right) + \frac{\partial}{\partial Z}\left(K\frac{\partial h}{\partial Z}\right) - \frac{\partial K}{\partial Z} - S, \tag{2}$$

where θ, K and S represent the soil water content, hydraulic conductivity, and root-water uptake function, respectively. In this equation, h denotes the suction potential. The root water uptake utilized in this study is based on the model presented in [41] and is defined as follows:

$$S(X, Z, h) = \gamma(h)\frac{L_t\beta(X,Z)T_{pot}}{\int\limits_0^{Z_m}\int\limits_{L+D-X_m}^{L+D}\beta(X,Z)dXdZ}. \tag{3}$$

The function γ is the dimensionless response function for soil water stress, and it is defined as follows [39]:

$$\gamma(h) = \begin{cases} -\frac{5}{8}h, & \text{for } -1.6 \le h \le 0 \\ 1, & \text{for } -4.7 < h < -1.6 \\ \frac{2}{7}h + \frac{82}{35}, & \text{for } -8.2 \le h \le -4.7 \end{cases}, \tag{4}$$

L_t represents the width of the soil surface related to the transpiration rate, T_{pot} stands for the potential transpiration, and β is the modeled spatial distribution of root-water uptake, defined as:

$$\beta(X,Z) = \left(1 - \frac{Z}{Z_m}\right)\left(1 - \frac{L+D-X}{X_m}\right)\exp(-K), \tag{5}$$

where

$$K = \frac{P_Z}{Z_m}|Z^* - Z| + \frac{P_X}{X_m}|X^* - (L + D - X)|.$$

In this context, the parameters P_Z, P_X, Z^*, and X^* are empirical in nature.

The flux normal to a surface with an outward-pointing normal vector $\mathbf{n} = (n_1, n_2)$ is described as per the reference [33]

$$F = Un_1 + Vn_2 = -K\left[\frac{\partial h}{\partial X}n_1 + \left(\frac{\partial h}{\partial Z} - 1\right)n_2\right]. \tag{6}$$

Utilizing Gardner's formula [16], [52],

$$K = K_s e^{\alpha h}, \tag{7}$$

where K_s represents the saturated hydraulic conductivity, and α is the soil parameter associated with the soil grain size, we obtain

$$\frac{\partial h}{\partial X} = \frac{1}{\alpha K}\frac{\partial K}{\partial X}, \tag{8}$$

$$\frac{\partial h}{\partial Z} = \frac{1}{\alpha K}\frac{\partial K}{\partial Z}, \tag{9}$$

and Equation (2) can be written as

$$\frac{\partial \theta}{\partial t} = \frac{1}{\alpha}\left(\frac{\partial^2 K}{\partial X^2} + \frac{\partial^2 K}{\partial Z^2}\right) - \frac{\partial K}{\partial Z} - S. \tag{10}$$

Flux normal (6) becomes

$$F = \left(-\frac{1}{\alpha}\frac{\partial K}{\partial X}\right)n_1 + \left(K - \frac{1}{\alpha}\frac{\partial K}{\partial Z}\right)n_2. \tag{11}$$

In the scenario of a time-independent infiltration problem, Equation (10) transforms into

$$\frac{\partial^2 K}{\partial X^2} + \frac{\partial^2 K}{\partial Z^2} - \alpha\frac{\partial K}{\partial Z} = S. \tag{12}$$

In this study, we are addressing time-independent infiltration problems into a two-layered soil with root-water uptake in the upper layer. Following the approach in [25], we have the system of differential equations to model these problems as

$$\frac{\partial^2 K_1}{\partial X^2} + \frac{\partial^2 K_1}{\partial Z^2} - \alpha_1\frac{\partial K_1}{\partial Z} = \alpha_1 S, \tag{13}$$

$$\frac{\partial^2 K_2}{\partial X^2} + \frac{\partial^2 K_2}{\partial Z^2} - \alpha_2\frac{\partial K_2}{\partial Z} = 0. \tag{14}$$

Here, K_1 and α_1 represent the hydraulic conductivity and the soil parameter of the upper layer, while K_2 and α_2 are the hydraulic conductivity and the soil parameter of the lower layer. The flux normal to the upper layer and the lower layer, with outward-pointing normals $\mathbf{n}1 = (n11, n_{21})$ and $\mathbf{n}2 = (n12, n_{22})$, is given by

$$F_1 = \left(-\frac{1}{\alpha_1}\frac{\partial K_1}{\partial X}\right)n_{11} + \left(K_1 - \frac{1}{\alpha_1}\frac{\partial K_1}{\partial Z}\right)n_{21}, \tag{15}$$

$$F_2 = \left(-\frac{1}{\alpha_2}\frac{\partial K_2}{\partial X}\right)n_{12} + \left(K_2 - \frac{1}{\alpha_2}\frac{\partial K_2}{\partial Z}\right)n_{22}, \tag{16}$$

respectively.

1) Interface conditions: The conditions at the interface layer are defined as [25], [28]

$$h_1 = h_2, \tag{17}$$

$$F_1 = -F_2, \tag{18}$$

at $Z = D_1$. Here h_1 is the soil water potential in the upper layer, and h_2 is the soil water potential in the lower layer.

From Equation (7), Equation (17) results in

$$K_2 = \frac{K_{s2}}{K_{s1}^{\alpha_2/\alpha_1}}K_1^{\alpha_2/\alpha_1}, \tag{19}$$

where K_{s1} is the saturated hydraulic conductivity of upper level soil and K_{s2} is the saturated hydraulic conductivity of lower level soil.

From Equation (7) and Equation (19), Equation (18) results in

$$\frac{\partial K_2}{\partial n} = \alpha_2\left(K_1 - \frac{K_{s2}}{K_{s1}^{\alpha_2/\alpha_1}}K_1^{\alpha_2/\alpha_1}\right) - \frac{\alpha_2}{\alpha_1}\frac{\partial K_1}{\partial n}. \tag{20}$$

2) Boundary conditions: Based on the boundary conditions outlined in the previous section and the interface conditions provided, utilizing Equation (15) and Equation (16), the boundary interface conditions in terms of K_1 and

K_2 are as follows

$$\frac{\partial K_1}{\partial n} = \alpha_1(v_0 + n_{21}K_1), \text{ on the channel's surface,} \tag{21}$$

$$\frac{\partial K_1}{\partial n} = -\alpha_1 K_1, \text{ for } \frac{2L}{\pi} < X < L+D \text{ and } Z = 0, \tag{22}$$

$$\frac{\partial K_1}{\partial n} = 0, \text{ for } X = 0 \text{ and } \frac{3L}{2\pi} < Z < D_1, \tag{23}$$

$$\frac{\partial K_1}{\partial n} = 0, \text{ for } X = L+D \text{ and } 0 < Z < D_1, \tag{24}$$

$$K_2 = \frac{K_{s2}}{K_{s1}^{\alpha_2/\alpha_1}} K_1^{\alpha_2/\alpha_1}, \text{ for } 0 < X < L+D$$
$$\text{and } Z = D_1, \tag{25}$$

$$\frac{\partial K_2}{\partial n} = \alpha_2 \left(K_1 - \frac{K_{s2}}{K_{s1}^{\alpha_2/\alpha_1}} K_1^{\alpha_2/\alpha_1} \right) - \frac{\alpha_2}{\alpha_1}\frac{\partial K_1}{\partial n},$$
$$\text{for } 0 < X < L+D \text{ and } Z = D_1, \tag{26}$$

$$\frac{\partial K_2}{\partial n} = 0, \text{ for } X = 0 \text{ and } D_1 < Z < D_1+D_2, \tag{27}$$

$$\frac{\partial K_2}{\partial n} = 0, \text{ for } X = L+D \text{ and } D_1 < Z < D_1+D_2, \tag{28}$$

and

$$K_2 = K_{s2}, \text{ for } 0 < X < L+D \text{ and } Z = D_1+D_2. \tag{29}$$

Therefore, the mathematical model for the infiltration problems in a two-layered soil, as considered in this study, is represented by the system of partial differential equations (13) and (14), taking into account the boundary interface conditions (21) to (29).

Equations (13) and (14) are two-dimensional diffusion-convection equations, and they can be solved numerically using the Dual Reciprocity Method (DRM) by reformulating the equations into

$$\lambda(\xi_1,\eta_1)K_1(\xi_1,\eta_1)$$
$$= \alpha_1 \iint\limits_{\Omega_1} \varphi(x,y;\xi_1,\eta_1)$$
$$\times \left[\frac{\partial}{\partial Z}(K_1(x,y)) + S(h,X,Z) \right] dxdy$$
$$+ \int\limits_{\Gamma_1} \left[K_1(x,y)\frac{\partial}{\partial n}(\varphi(x,y;\xi_1,\eta_1)) \right.$$
$$\left. - \varphi(x,y;\xi_1,\eta_1)\frac{\partial}{\partial n}(K_1(x,y)) \right] ds, \tag{30}$$

and

$$\lambda(\xi_2,\eta_2)K_2(\xi_2,\eta_2)$$
$$= \alpha_2 \iint\limits_{\Omega_2} \varphi(x,y;\xi_2,\eta_2)\frac{\partial}{\partial Z}(K_2(x,y))dxdy$$
$$+ \int\limits_{\Gamma_2} \left[K_2(x,y)\frac{\partial}{\partial n}(\varphi(x,y;\xi_2,\eta_2)) \right.$$
$$\left. - \varphi(x,y;\xi_2,\eta_2)\frac{\partial}{\partial n}(K_2(x,y)) \right] ds, \tag{31}$$

where $\varphi(x,y;\xi,\eta)$ is the fundamental solution of two-dimensional Laplace equation, and

$$\lambda(\xi_i,\eta_i) = \begin{cases} 1/2, & (\xi_i,\eta_i) \text{ lies on smooth part of } \Gamma_i \\ 1, & (\xi_i,\eta_i) \in \Omega_i \end{cases},$$
$$\text{for } i = 1,2. \tag{32}$$

To apply the Dual Reciprocity Method (DRM), we discretize Γ_1 and Γ_2 into a set of elements, and we select a number of interior points within Ω_1 and Ω_2. Let N_1 and N_2 represent the number of elements on Γ_1 and Γ_2, and let M_1 and M_2 denote the number of interior collocation points within Ω_1 and Ω_2. Utilizing these elements and interior points, the integral equations (30) and (31) are reformulated into a system of linear algebraic equations as follows

$$\lambda^{(n_1)}K_1^{(n_1)} = \sum_{j=1}^{N_1} \left(\mathfrak{F}_{2,1}^{(n_1 j)}K_1^{(j)} - \mathfrak{F}_{1,1}^{(n_1 j)}\bar{K}_1^{(j)} \right)$$
$$+ \alpha_1 \sum_{j=1}^{N_1+M_1} \mu_1^{(n_1 j)} \left[S\left(K_1^{(i)}, a_1^{(i)}, b_1^{(i)}\right) \right.$$
$$\left. + \sum_{m=1}^{N_1+M_1} \bar{\rho}_Z^{(jm)} \left(\sum_{i=1}^{N_1+M_1} \omega_1^{(mi)}K_1^{(i)} \right) \right],$$
$$\text{for } n_1 = 1,2,\cdots,N_1+M_1, \tag{33}$$

and

$$\lambda^{(n_2)}K_2^{(n_2)} = \sum_{k=1}^{N_2} \left(\mathfrak{F}_{2,2}^{(n_2 k)}K_2^{(k)} - \mathfrak{F}_{1,2}^{(n_2 k)}\bar{K}_2^{(k)} \right)$$
$$+ \alpha_2 \sum_{k=1}^{N_2+M_2} \mu_2^{(n_2 k)}$$
$$\times \left[\sum_{l=1}^{N_2+M_2} \bar{\rho}_Z^{(kl)} \left(\sum_{i=1}^{N_2+M_2} \omega_2^{(li)}K_2^{(i)} \right) \right],$$
$$\text{for } n_2 = 1,2,\cdots,N_2+M_2. \tag{34}$$

Here $(a_1^{(i)}, b_1^{(i)})$, $i = 1,2,\cdots,N_1+M_1$ be the collocation points on Γ_1 and in Ω_1, $(a_2^{(k)}, b_2^{(k)})$, $k = 1,2,\cdots,N_2+M_2$ be the collocation points on Γ_2 and in Ω_2, $\lambda^{(n_1)} = \lambda(a_1^{(n_1)}, b_1^{(n_1)})$, $\lambda^{(n_2)} = (a_2^{(n_2)}, b_2^{(n_2)})$, $K_1^{(n_1)} = K_1(a_1^{(n_1)}, b_1^{(n_1)})$, $K_2^{(n_2)} = K_2(a_2^{(n_2)}, b_2^{(n_2)})$, $\bar{K}_1^{(n_1)} = (\partial K_1/\partial n)|_{(x,y)=(a_1^{(n_1)},b_1^{(n_1)})}$, $\bar{K}_2^{(n_2)} = (\partial K_2/\partial n)|_{(x,y)=(a_2^{(n_2)},b_2^{(n_2)})}$,

$$\mathfrak{F}_{1,1}^{(n_1 j)} = \int\limits_{C_1^{(j)}} \varphi(x,y;a_1^{(n_1)}, b_1^{(n_1)})ds(x,y),$$

$$\mathfrak{F}_{1,2}^{(n_2 j)} = \int\limits_{C_2^{(j)}} \varphi(x,y;a_2^{(n_2)}, b_2^{(n_2)})ds(x,y),$$

$$\mathfrak{F}_{2,1}^{(n_1 j)} = \int\limits_{C_1^{(j)}} \frac{\partial}{\partial n}\left[\varphi(x,y;a_1^{(n_1)}, b_1^{(n_1)})\right]ds(x,y),$$

$$\mathfrak{F}_{2,2}^{(n_2 j)} = \int\limits_{C_2^{(j)}} \frac{\partial}{\partial n}\left[\varphi(x,y;a_2^{(n_2)}, b_2^{(n_2)})\right]ds(x,y).$$

The notation $\rho^{(mk)}$ is defined as

$$\rho^{(mk)} = \rho(a^{(m)}, b^{(m)}; a^{(k)}, b^{(k)}) = 1 + \left(r^{(mk)}\right)^2 + \left(r^{(mk)}\right)^3,$$

where $r^{(mk)} = \sqrt{\left(a^{(m)} - a^{(k)}\right)^2 + \left(b^{(m)} - b^{(k)}\right)^2}$. The symbol $\bar{\rho}_Z^{(jm)}$ denotes

$$\frac{\partial}{\partial Z}\left(\rho(a^{(j)}, b^{(j)}; x, y)\right)\Big|_{(x,y)=(a^{(m)},b^{(m)})}.$$

The coefficients $\omega_1^{(mk)}$ and $\omega_2^{(nk)}$ are defined as

$$\sum_{i=1}^{N_1+L_1} \omega_1^{(mi)}\rho^{(ik)} = \begin{cases} 1, & \text{if } m = k \\ 0, & \text{if } m \neq k \end{cases},$$

$$\sum_{i=1}^{N_2+L_2} \omega_2^{(ni)}\rho^{(ik)} = \begin{cases} 1, & \text{if } n = k \\ 0, & \text{if } n \neq k \end{cases}.$$

Two numbers $\mu_1^{(n_1 j)}$ and $\mu_2^{(n_2 j)}$ are defined as

$$\mu_1^{(n_1 j)} = \sum_{k=1}^{N_1+L_1} h_1^{(n_1 k)}\omega_1^{(kj)},$$

$$\text{and } \mu_2^{(n_2 j)} = \sum_{k=1}^{N_2+L_2} h_2^{(n_2 k)}\omega_2^{(kj)},$$

where

$$h_1^{(n_1 k)} = \lambda^{(n_1)}\chi(a_1^{(n_1)}, b_1^{(n_1)}, a_1^{(k)}, b_1^{(k)})$$
$$+ \sum_{j=1}^{N_1}\left[\frac{\partial}{\partial n}\left(\chi(x, y; a_1^{(j)}, b_1^{(j)})\right)\right]\Big|_{(x,y)=(a_1^{(k)}, b_1^{(k)})}$$
$$\times \mathfrak{F}_{1,1}^{(nj)}$$
$$- \sum_{j=1}^{N}\chi(a_1^{(k)}, b_1^{(k)}; a_1^{(j)}, b_1^{(j)})\mathfrak{F}_{2,1}^{(nj)},$$

$$h_2^{(n_2 k)} = \lambda^{(n_2)}\chi(a_2^{(n_2)}, b_2^{(n_2)}, a_2^{(k)}, b_2^{(k)})$$
$$+ \sum_{j=1}^{N_2}\left[\frac{\partial}{\partial n}\left(\chi(x, y; a_2^{(j)}, b_2^{(j)})\right)\right]\Big|_{(x,y)=(a_2^{(k)}, b_2^{(k)})}$$
$$\times \mathfrak{F}_{1,2}^{(nj)}$$
$$- \sum_{j=1}^{N}\chi(a_1^{(k)}, b_1^{(k)}; a_1^{(j)}, b_1^{(j)})\mathfrak{F}_{2,2}^{(nj)},$$

and χ is a function satisfying

$$\frac{\partial^2 \chi}{\partial x^2} + \frac{\partial^2 \chi}{\partial y^2} = \rho.$$

Let n_0 be the number of elements on the interface. In System of equations (33), when j varies from $N_0 + 1$ to $N_0 + n_0$, both K_1 and $\bar{K}_1$ are unknown variables. As a result, the total number of unknowns in equation (33) becomes $N_1 + M_1 + n_0$. Similarly, the number of unknowns in equation (34) is $N_2 + M_2 + n_0$. Consequently, solving the system of linear algebraic equations represented by (33) and (34) may not be feasible, as the number of provided equations is $N_1 + M_1$ and $N_2 + M_2$.

To overcome this issue, we incorporate the interface conditions (19) and (20), which allows us to express the system of linear algebraic equations (34) as follows

$$\lambda^{(n_2)}\kappa^{(n_2)}$$
$$= \sum_{j=1}^{n_0}\left\{\mathfrak{F}_{2,2}^{(n_2 j)}\frac{K_{s2}}{K_{s1}^{\alpha_2/\alpha_1}}\left[K_1^{(N_0+n_0+1-j)}\right]^{\alpha_2/\alpha_1}\right.$$
$$- \mathfrak{F}_{1,2}^{(n_2 j)}\left[\alpha_2\left(K_1^{(N_0+n_0+1-j)} - \frac{K_{s2}}{K_{s1}^{\alpha_2/\alpha_1}}\right.\right.$$
$$\times \left[K_1^{(N_0+n_0+1-j)}\right]^{\alpha_2/\alpha_1}\right)$$
$$\left.\left.- \frac{\alpha_2}{\alpha_1}\bar{K}_1^{(N_0+n_0+1-j)}\right]\right\}$$
$$+ \sum_{j=n_0+1}^{N_2}\left(\mathfrak{F}_{2,2}^{(n_2 j)}K_2^{(j)} - \mathfrak{F}_{1,2}^{(n_2 j)}\bar{K}_2^{(j)}\right)$$
$$+ \alpha_2\sum_{j=1}^{n_0}\mu^{(n_2 j)}\left[\sum_{m=1}^{N_2+M_2}\bar{\rho}_Z^{(jm)}\left(\sum_{i=1}^{n_0}\omega_2^{(mi)}\frac{K_{s2}}{K_{s1}^{\alpha_2/\alpha_1}}\right.\right.$$
$$\left.\left.\times \left[K_1^{(N_0+n_0+1-i)}\right]^{\alpha_2/\alpha_1}\right)\right],$$
$$+ \alpha_2\sum_{j=n_0+1}^{N_2+M_2}\mu^{(n_2 j)}$$
$$\times \left[\sum_{m=1}^{N_2+M_2}\bar{\rho}_Z^{(jm)}\left(\sum_{i=n_0+1}^{N_2+M_2}\omega_2^{(mi)}K_2^{(i)}\right)\right],$$
$$\text{for } n_2 = 1, 2, \cdots, N_2 + M_2. \tag{35}$$

It can be seen that (35) is not a system of linear algebraic equations. Here

$$\kappa^{(n_2)} = \begin{cases} K^*\left[K_1^{(N_0+n_0+1-n_2)}\right]^{\alpha}, & \text{for } n_2 = 1, 2, ..., n_0 \\ K_2^{(n_2)}, & \text{for } n_2 = n_0 + 1, n_0 + 2, ..., N_2 + M_2 \end{cases},$$

where $\alpha = \alpha_2/\alpha_1$ and $K^* = K_{s2}/(K_{s1})^{\alpha}$.

Now, in the system of linear algebraic equations (33) and the system of algebraic equations (35), the number of unknowns is $N_1 + N_2 + M_1 + M_2$, and the number of equations matches the number of unknowns. Therefore, solutions can be obtained by solving these systems of equations simultaneously.

However, it's worth noting that the system of equations (35) is not a system of linear algebraic equations. Therefore, before solving these two systems of equations, we need to transform (35) into a system of linear algebraic equations using the following iterative steps

1) Equation (13) with respect to boundary conditions

$$\frac{\partial K_1}{\partial n} = \alpha_1(v_0 + n_2 K_1), \text{ on the channel's surface,}$$
$$\frac{\partial K_1}{\partial n} = -\alpha_1 K_1, \text{ for } \frac{2L}{\pi} < X < L \text{ and } Z = 0,$$
$$\frac{\partial K_1}{\partial n} = 0, \text{ for } X = 0 \text{ and } 0 < Z < D_1,$$
$$\frac{\partial K_1}{\partial n} = 0, \text{ for } X = L \text{ and } 0 < Z < D_1,$$
$$K_1 = K_{s1}, \text{ for } 0 < X < L \text{ and } Z = D_1 + D2,$$

is solved using the Dual Reciprocity Method (DRM) to obtain numerical values for K_1. Likewise, Equation (14) is solved to obtain the value of K_2.

2) At the interface $Z = D_1$, the initial predictions of K are computed according to the formula defined in the following equation

$$K^*{}_{(0)}{}^{(i)} = \sqrt{K_1{}^{(N+M_1+i)} K_2{}^{(N+M_1+i)}},$$
$$i = 1, 2, \cdots, n_0. \qquad (36)$$

Here, N represents the number of line segments, M_1 is the count of selected interior points for $Z < D_1$, and n_0 is the number of interior points at $Z = D_1$. Formula (36) is borrowed from [17].

3) At the k-th iteration, the nonlinear terms $[K_1{}^{(N_0+n_0+1-i)}]^{\alpha_2/\alpha_1}$, where i ranges from 1 to n_0, are estimated using a Taylor polynomial expansion around $K^*{}_{(k-1)}{}^{(i)}$, and this is given by

$$\begin{aligned}
\left[K_1{}^{(N_0+n_0+1-i)}\right]^{\frac{\alpha_2}{\alpha_1}} &\approx \left[K^*{}_{(k-1)}{}^{(i)}\right]^{\frac{\alpha_2}{\alpha_1}} \\
&+ \frac{\alpha_2}{\alpha_1}\left[K^*{}_{(k-1)}{}^{(i)}\right]^{\left[\frac{\alpha_2}{\alpha_1}-1\right]} \\
&\times \left(K_1{}^{(N_0+n_0+1-i)} \right. \\
&\left. -K^*{}_{(k-1)}{}^{(i)}\right). \quad (37)
\end{aligned}$$

In this context, $K^*{}_{(k-1)}{}^{(i)}$, where i ranges from 1 to n_0, represents the values of K on the interface at the $(k-1)$-th iteration.

4) The nonlinear terms in (35) are replaced with linear terms through the approximation given in (37). Subsequently, the system of algebraic equations (33) and (35) can be solved to obtain the values of K_1, K_2, $\bar{K}_1$, and $\bar{K}_2$.

5) We establish $K^*{}_{(k)}{}^{(i)} = K_1{}^{(N_0+n_0+1-i)}$, $i = 1, 2, \cdots, n_0$.

6) The value

$$d = \max\{|K^*{}_{(k)}{}^{(i)} - K^*{}_{(k-1)}{}^{(i)}| : i = 1, 2, \cdots, n_0\} \qquad (38)$$

is subsequently calculated.

7) If the value of d is not adequately small, we repeat steps 3) to 6) until we achieve the condition of convergence, represented by

$$d < \varepsilon \qquad (39)$$

where ε is a sufficiently small positive number. This inequality (39) signifies a convergence criterion.

The numerical values of K_1, K_2, $\bar{K}_1$, and $\bar{K}_2$ in step 4) are then used to obtain K_1 and K_2 at any points in $\Omega_1 \cup \Omega_2 \cup \Gamma_1 \cup \Gamma_2$.

IV. Results and discussion

The technique or method outlined in the previous section is applied to address steady infiltration problems from periodic trapezoidal channels into soils comprising two distinct layers with four different root-water uptake characteristics. The cross-sectional length of the channel and the bed's cross-section both measure 1 meter. The fluxes across the channel surfaces are assumed to be constant and denoted as v_0. The value of v_0 is specified as:

$$v_0 = 0.75 \times 0.099 \text{ m/day},$$

where 0.099 m/day represents the saturated hydraulic conductivity of Pima Clay Loam. The selection of this v_0 value follows a similar approach as that in [45]. Additionally, we set ϵ to be 10^{-4}. In this study, we deal with two different soil types: Pima Clay Loam (PCL), and Guelph Loam (GL). The values of K_s and α for these soils are summarized in Table I.

TABLE I: Soil's parameters.

	PCL	GL
K_s (m/day)	0.099	0.3171
α (m^{-1})	1.4	3.4

The values of the saturated hydraulic conductivity (K_s) and the soil parameter (α) employed in this paper are the same as those in [45]. Regarding the root-water uptake function, we have adopted parameters such as the root zone's depth, width, and other relevant factors from one of the models proposed in [49], which are outlined in Table II.

TABLE II: Root-water uptake function's parameters.

	Root A	Root B	Root C	Root D
X_m (m)	0.5	0.5	0.5	0.5
Z_m (m)	1.0	1.0	1.0	1.0
L_t (m)	0.5	0.5	0.5	0.5
T_{pot} (m/day)	0.004	0.004	0.004	0.004
P_Z	1.0	1.0	1.0	1.0
P_X	1.0	1.0	1.0	1.0
Z^* (m)	0.0	0.2	0.0	0.2
X^* (m)	1.0	1.0	0.75	0.75

Within Table II, X_m represents half the width of the root zone, Z_m signifies the depth of the root zone, L_t denotes half the length of the soil surface relevant to the transpiration process, T_{pot} stands for the transpiration potential, and P_Z, P_X, Z^*, and X^* are parameters related to root-water uptake.

The numerical method described is then implemented to solve steady infiltration problems with root-water uptake in two-layered soils GL-PCL. The upper layer is GL with depth of 2 m, and the lower layer is PCL with depth of 3 m. Four different root-uptakes are considered in this study. The root-water uptakes are as those summarized in Table II. To obtain numerical results, the numbers of elements for the upper and the lower layer are $N_1 = 67$ and $N_2 = 89$, respectively. For the number of interior points in the upper layer is $M_1 = 361$ and that in the lower layer is the same, $M_2 = 361$. These values of N_1, N_2, M_1 and M_2 are the same as those in [45].

Using the specified parameters, elements, and interior points mentioned earlier, we applied the IDRM method introduced in the previous section to obtain numerical solutions. The numerical results were achieved by conducting two iterations for all four cases of different types of root-water uptake. Notably, there were variations in the values of d among these cases. In this context, d represents the maximum difference between numerical K values obtained from consecutive iterations. The iteration process was terminated when d fell below the threshold of $\epsilon = 10^{-4}$.

For the Root A case, the d value equaled 0.000016, while for Root B, it was 0.000015. In the cases of Root C and Root D, the respective d values were 0.000013 and 0.000011. Selected results are displayed in Figure 1 through Figure 3.

(a) $X = 0.1$

(b) $X = 0.35$

(c) $X = 0.65$

(d) $X = 0.9$
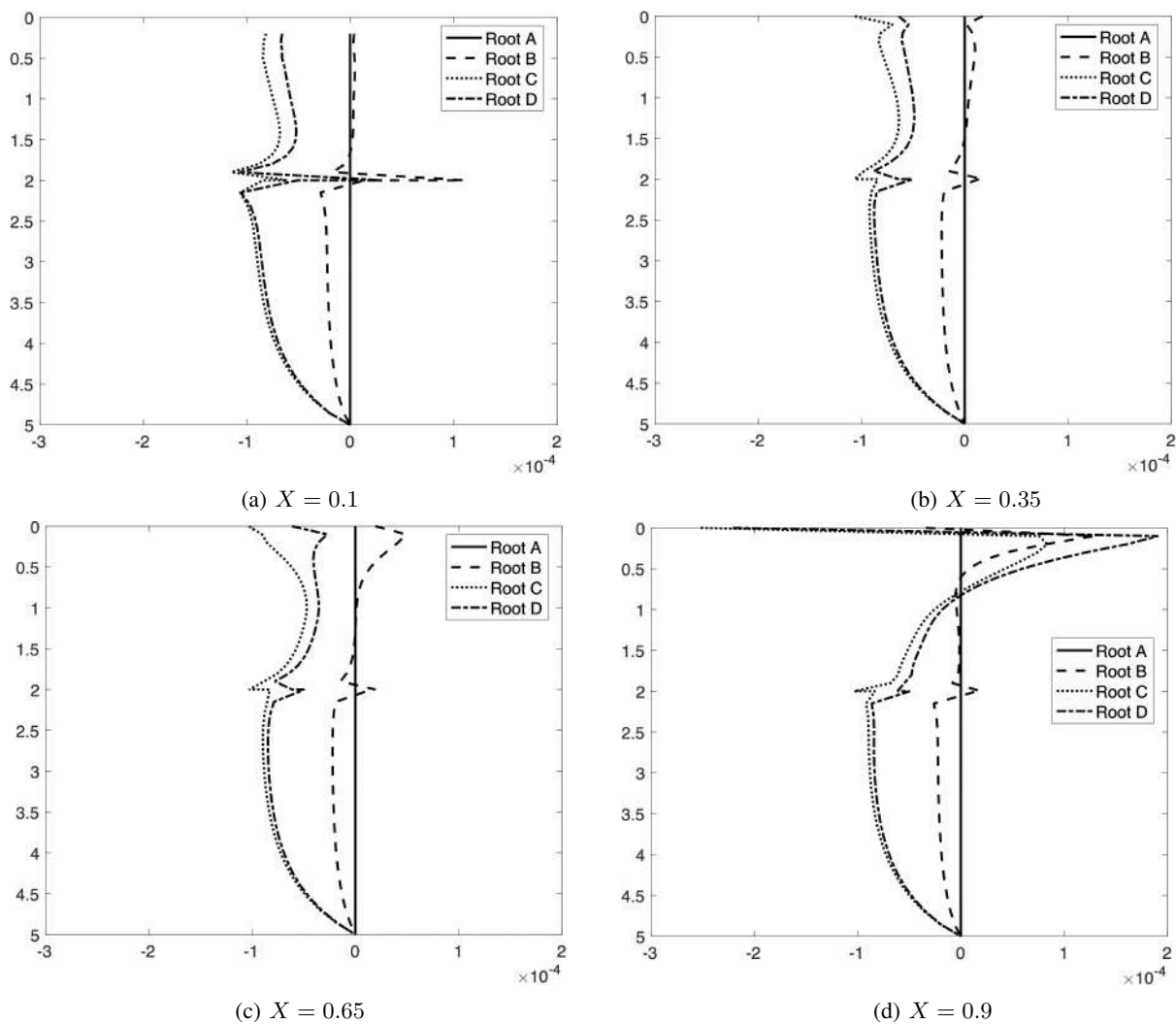
Fig. 1: Graphs of D_K along Z-axis (vertical axis) at selected values of X for the four different cases.

Figure 1 shows values of D_K along Z-axis at four selected values of X. Here, D_K is defined as

$$D_K(X, Z) = K(X, Z) - K_A(X, Z), \qquad (40)$$

where $K(X, Z)$ is the value of K at point (X, Z) and $K_A(X, Z)$ is the value of K for the Root A case at point (X, Z). As observed in Figure 1, it becomes evident that the values of D_K lie within the range of -1×10^{-4} to 1×10^{-4} for X values of 0.1, 0.35, and 0.65. However, for X equal to 0.9, the D_K values span from -3×10^{-4} to 2×10^{-4}, specifically at the soil surface within the root zone. These results indicate that the most significant disparities in K values are concentrated within the root zone. Consequently, these findings highlight that the discrepancies in K values among the four different cases under consideration are all below 3×10^{-4}.

In Figure 2, we observe the plots of S obtained from four different root uptake scenarios within the root zone, each corresponding to four distinct X values. Figure 2(a) displays the S plots at $X = 0.6$, while Figures 2(b), 2(c), and 2(d) depict the S plots at $X = 0.7, 0.8$, and 0.9, respectively.

It is evident that as X increases, S also experiences an increase. Furthermore, it is notable that the most significant uptake occurs at the soil surface. Root A and Root C exhibit similar S patterns, while Root B and Root D demonstrate analogous S behaviors.

At X values of 0.6, 0.7, and 0.8, the root uptakes from Root A are lower than those from Root C. This difference can be attributed to these X values being closer to 0.75, which is the X^* value for Root C, rather than 1.00, which is the X^* value for Root A. However, at $X = 0.90$, Root A results in higher S compared to Root C, as 0.90 is closer to 1.00 than 0.75.

At $X = 0.6$, near the soil surface, the range of root uptake falls between 0.001 and 0.003. Among the roots, Root C yields the highest S value at the surface, while Root B results in the lowest root uptake. Moving on to $X = 0.7$, near the soil surface, S spans from 0.003 to 0.007. The pattern of S distribution at $X = 0.7$ mirrors that at $X = 0.6$.

At $X = 0.8$, in the vicinity of the soil surface, root uptake varies from 0.0068 to 0.0115. However, the distribution of S at $X = 0.8$ differs from the previous two plots. Finally, at $X = 0.9$, near the soil surface, root uptake falls within the range of 0.01 to 0.016. Moreover, the distribution pattern of S is distinct from the previous three scenarios.

Figure 3 provides mesh plots illustrating root-water uptake for four distinct root types. Specifically, Figure 3(a) represents Root A, Figure 3(b) illustrates Root B, Figure 3(c) depicts Root C, and Figure 3(d) showcases Root D. It is
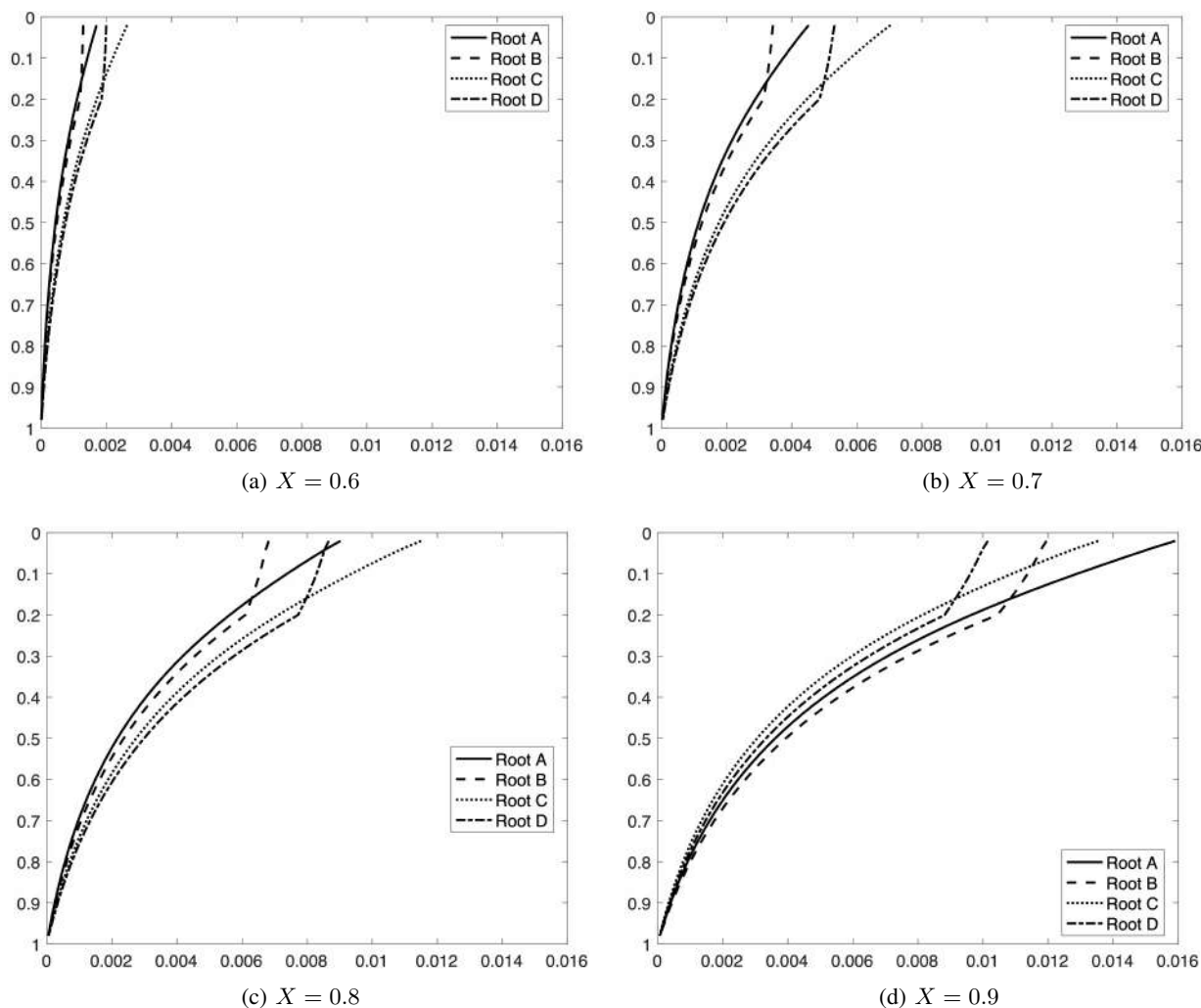
Fig. 2: Plots of S along Z-axis (vertical axis) at selected values of X in the root zone for the four different cases.

notable that Root A yields the highest water uptake value, located precisely at point (1.00, 0.00). This outcome can be explained by the position of (X^*, Z^*) and the soil water stress value, denoted as $\gamma(h)$. The point (X^*, Z^*) aligns at coordinates (1.00, 0.00), and the $\gamma(h)$ value at this point is the highest compared to other points. However, the root-water uptake values rapidly decrease beyond a depth of 0.4 meters ($Z > 0.4$ m), becoming lower than those resulting from the other root types.

Furthermore, it's evident that there are distinct folds in Figures 3(b), 3(c), 3(d). In Figure 3(b), the fold occurs at $Z = 0.2$. For Figure 3(c), the fold is positioned at $X = 0.75$. In Figure 3(d), folds are noticeable at both $X = 0.75$ and $Z = 0.2$. These findings highlight that these folds are situated precisely at X^* and Z^*.

In addition, the total uptake are computed numerically. To compute the total uptake, the root zone is divided into 50×50 equal regions. Let (X_{ij}, Z_{ij}) be the top right corner of the region at i-th row and j-th collumn. The total uptake (TU) is computed using the formula

$$TU = \sum_{i=1}^{50} \sum_{j=1}^{50} S(X_{ij}, Z_{ij}, h_{ij}), \qquad (41)$$

where h_{ij} is the suction potential at the top right corner at

i-th row and j-th collumn. Results obtained using Equation (41) are summarized in Table III.

TABLE III: Total water uptake from different types of root uptake.

	Root A	Root B	Root C	Root D
Total uptake (m^3/day)	0.00133415	0.00132069	0.00132834	0.00131629

From Table III, it can be seen that all the types of root give about similar amount of water absorbed. In particular, Root A uptakes 0.00133415 cubic meters per day or 1334.15 cubic centimeters per day, Root B uptakes approximately 1320.69 cubic centimeters per day, Root C uptakes roughly 1328.34 cubic centimeters per day, and Root D uptakes 1316.29 cubic centimeters per day. From these results, it is apparent that roots with (X^*, Z^*) (the point with the highest absorption value) closest to the stem of the plant produce a greater total absorption compared to roots with (X^*, Z^*) further away from the stem.

(a) Root A

(b) Root B

(c) Root C

(d) Root D
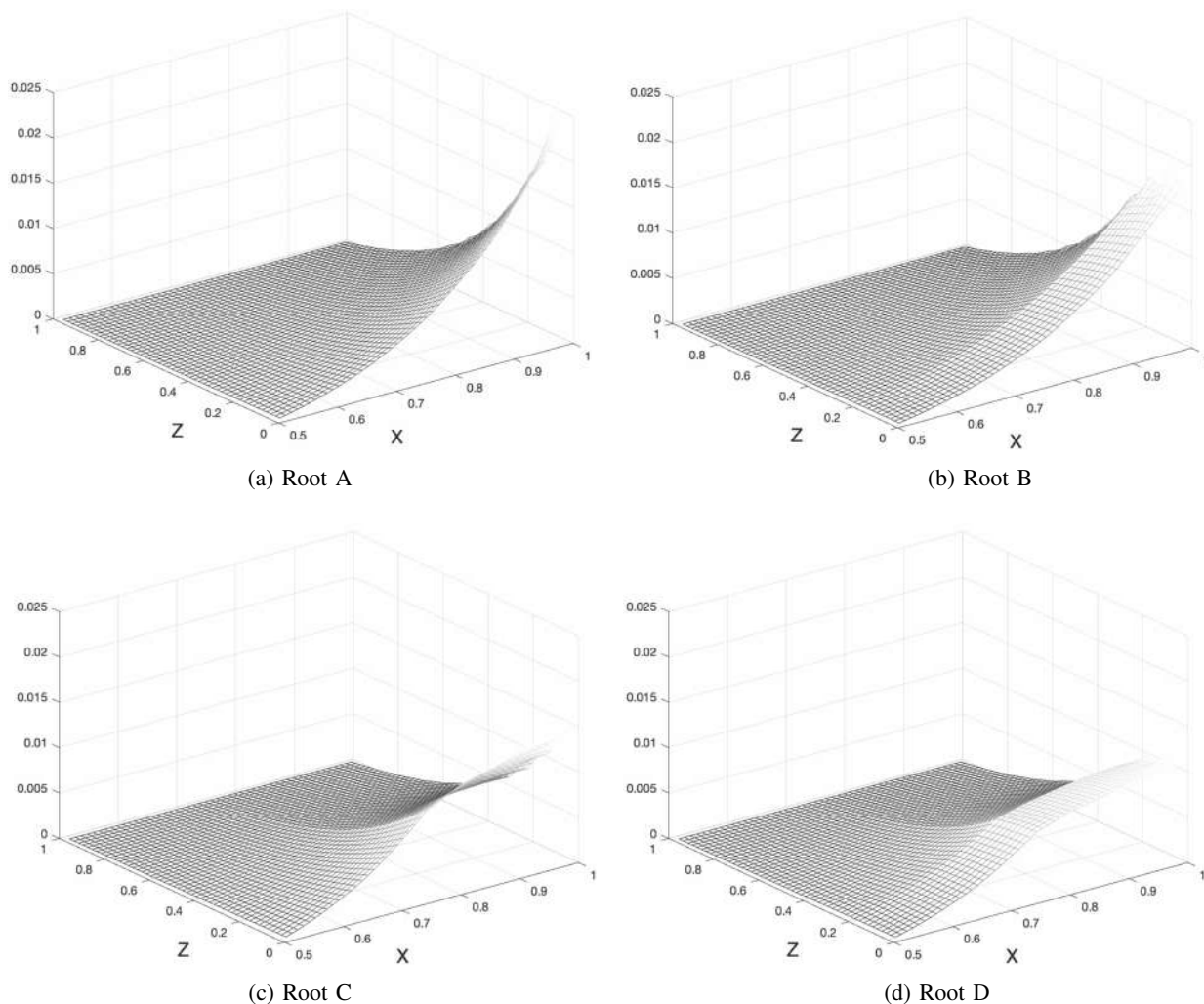
Fig. 3: Mesh plots of S over the root zone.

V. CONCLUDING REMARKS

A mathematical model has been developed to describe the steady infiltration process from periodic trapezoidal channels into soils with two distinct layers, taking into account root-water uptake. This model has been effectively solved through numerical techniques, employing an Iterative Dual Reciprocity Method (IDRM). Using the IDRM, we have obtained numerical solutions for hydraulic conductivity and computed numerical values for soil water potential. To assess the method's performance, we have conducted tests on four different problems.

The findings from our analysis reveal that the hydraulic conductivity and soil water potential in the lower layer are primarily influenced by the properties of the soil in that lower layer. Conversely, in the upper soil layer, the values of these parameters are predominantly influenced by the type of soil present at the surface.

Regarding soil water potential, these values exhibit a trend of either increasing or decreasing as they approach the suction potential in the lower layer at the interface. Furthermore, the values of hydraulic conductivity correspond to the values of either the suction potential or the soil water potential. Furthermore, roots with highest absorption point closer to the plant's stem, absorb more water compared to those with highest absorption point located farther away from the stem.

REFERENCES

[1] Amoozegar-Fard A, Warrick AW, Lomen DO. Design nomographs for trickle irrigation system. J. Irrig. Drain. Eng. 1984; 110: 107 - 120.

[2] Azis MI, Clements DL, Lobo M. A boundary element method for steady infiltration from periodic channels. ANZIAM J. 2003; 44(E): C61 – C78.

[3] Barontini S, Ranzi R, Bacchi B. Water dynamics in a gradually nonhomogeneous soil described by linearized Richards equation. Water Resour. Res. 2007; 43(8): W08411.

[4] Basha HA. Multidimensional linearized nonsteady infiltration with prescribed boundary conditions at the soil surface. Water Resour. Res. 1999; 35(1): 75 - 83.

[5] Basha HA. Multidimensional linearized nonsteady infiltration toward a shallow water table. Water Resour. Res. 2000; 36(9): 2567 - 2573.

[6] Batu V. Steady infiltration from single and periodic strip sources. Soil Sci. Soc. Am. J. 1978; 42: 544 - 549.

[7] Belfort B, Lehmann F. Comparison of equivalent conductivities for numerical simulation of one-dimensional unsaturated flow. Vadoze Zone J. 2005; 4(4): 1191 - 1200.

[8] Brunone B, Ferrante M, Romano N, Santini A. Numerical simulations of one-dimensional infiltration into layered soils with the Richard's equation using different estimates of the interlayer conductivity. Vadoze Zone J. 2003; 2(2): 193 - 200.

[9] Bresler E. Analysis of trickle irrigation with application to design problems. Irrigation Science. 1978; 1: 3 - 17.

[10] Celia M, Bouloutas E, Zarba R. A general mass-conservative numerical solution for the unsaturated flow equation. Water Resour. Res. 1990; 26(7): 1483 - 1496.

[11] Chen G, Gallipoli D. Steady infiltration from buried point source into heterogeneous cross-anisotropic unsaturated soil. International Journal for Numerical and Analytical Methods in Geomechanics. 2004; 28: 1033 - 1055.

[12] Clements DL, Lobo M. A BEM for time dependent infiltration from an irrigation channel. Eng. Anal. Bound. Elem. 2010; 34(12): 1100 - 1104.

[13] Diaw EB, Lehmann F, Ackerer P. One-dimensional simulation of solute transfer in saturated–unsaturated porous media using the discontinuous finite elements method. Journal of Contaminant Hydrology. 2001; 51(3-4): 197 - 213.

[14] Farthing MW, Kees CE, Miller CT. Mixed finite element methods and higher-order temporal approximations. Advances in Water Resources. 2002; 25(1): 85 - 101.

[15] Farthing MW, Ogden FL. Numerical solution of Richards' equation: A review of advances and challenges. Soil Sci. Soc. Am. J. 2017; 81: 1257 − 1269.

[16] Gardner WR. Some steady-state solutions to the unsaturated moisture flow equation with application to evaporation from a water table. Soil Sci. 1958; 85: 228 - 232.

[17] Haverkamp R, Vauclin M. A note on estimating finite difference interblock hydraulic conductivity values for transient unsaturated flow problems. Water Resour. Res. 1979; 15: 181 - 187.

[18] Katsikadelis JT. Boundary elements: Theory and applications. Elsevier, Amsterdam-London-New York-Oxford-Paris-Tokyo-Boston-San Diego-San Francisco-Singapore-Sydney, 2002.

[19] Li KY, De-Jong R, Boisvert JB. An exponential root-water uptake model with water stress compensation. Journal of Hydrology. 2001; 252: 189 - 204.

[20] Li H, Farthing M, Dawson C, Miller CT. Local discontinuous Galerkin approximations to Richards equation. Adv. Water Resour. 2007; 30(3): 555 - 575.

[21] Li H, Farthing M, Miller CT. Adaptive local discontinuous Galerkin approximations to Richards equation. Adv. Water Resour. 2007; 30(9): 1883 - 1901.

[22] Lima-Vivancos V, Voller V. Two numerical methods for modelling variably saturated flow in layered media. Vadose Zone J. 2004; 3(3): 1031 - 1037.

[23] List F, Radu FA. A study on iterative methods for solving Richards' equation. Comput. Geosci. 2016; 20: 341 − 353.

[24] Lobo M, Clements DL, Widana N. Infiltration from irrigation channels in a soil with impermeable inclussions. ANZIAM J. 2005; 46: C1055 - C1068.

[25] De Luca DL, Cepeda JM. Procedure to obtain analytical solutions of one-dimensional Richard's equation for infiltration in two-layered soils. Journal of Hydrol. Eng. 2016; 21(7): 04016018.

[26] Lomen DO, Warrick AW. Time Dependent Linearized Infiltration. II. Line Sources. Soil Science Society of America Proceedings. 1974; 38: 568 - 572.

[27] Mandal AC, Waechter RT. Steady Infiltration in Unsaturated Soil from a Buried Circular Cylinder: The Separate Contributions from Top and Bottom Halves. Water Resour. Res. 1994; 30: 107 - 115.

[28] Matthews CJ, Braddock RD, Sander GC. Modeling flow through a one-dimensional multi-layered soil profile using the method of lines. Environmental Modeling and Assessment. 2004; 9: 103 - 113.

[29] Oldenburg CM, Pruess K. On numerical modeling of capillary barriers. Water Resour. Res. 1993; 29(4): 1045 - 1056.

[30] Pall R, Jarret AR, Morrow CT. Transient soil moisture movement through layered soils using a finite element approach. Transactions of the ASAE. 1981; 24(3): 678 - 683.

[31] Peters A, Durner W, Idenb SC. Modified Feddes type stress reduction function for modeling root water uptake: Accounting for limited aeration and low water potential. Agricultural Water Management. 2017; 185: 126 − 136.

[32] Philip JR. Steady Infiltration from Buried Point Sources and Spherical Cavities. Water Resour. Res. 1968; 4: 1039 - 1047.

[33] Philip JR. Flow in porous media. Annu. Rev. Fluid Mech. 1970; 2: 177 - 204.

[34] Philip JR. Steady infiltration from buried, surface, and perched point and line sources in heterogeneous soils: I. Analysis. Soil Science Society American Proceeding. 1972; 36: 268 - 273.

[35] Philip JR. Steady infiltration from circular cylindrical cavities. Soil Science Society of America Journal. 1984; 48(2): 270 - 278.

[36] Philip JR. The scattering analog for infiltration in porous media. Rev. of Geophysics. 1989; 27(4): 431 - 448.

[37] Pullan AJ. Linearized time-dependent infiltration from a shallow pond. Water Resour. Res. 1992; 28(4): 1041 - 1046.

[38] Ross PJ, Bristow KL. Simulating water movement in layered and gradational soils using the Kirchhoff transform. Soil Sci. Soc. Am. J. 1990; 54(6): 1519 - 1524.

[39] Solekhudin I, Ang KC. A DRBEM with a predictor–corrector scheme for steady infiltration from periodic channels with root-water uptake. Eng. Anal. Bound. Elem. 2012; 36: 1199 - 1204.

[40] Solekhudin I, Ang KC. A DRBEM for time-dependent infiltration from periodic irrigation channels in a homogeneous soil. Electronic Journal of Bound. Elem. 2013; 11(1): 1 - 12.

[41] Solekhudin I, Ang KC. A Laplace transform DRBEM with a predictor–corrector scheme for time-dependent infiltration from periodic channels with root-water uptake. Engineering Analysis with Boundary Elements. 2015; 50: 141 - 147.

[42] Solekhudin I. Water infiltration from periodic trapezoidal channels with different types of root-water uptake. Far East Journal of Mathematical Sciences. 2016; 100(12): 2029 - 2040.

[43] Solekhudin I. A numerical method for time-dependent infiltration from periodic trapezoidal channels with different types of root-water uptake. IAENG International Journal of Applied Mathematics. 2018; 48(1): 84 - 89.

[44] Solekhudin I, Purnama D, Malysa NH, Sumardi. Characteristics of water flow in heterogeneous soils. JP Journal of Heat and Mass Transfer. 2018; 15(3): 597 - 608.

[45] Solekhudin I. Boundary interface water infiltration into layered soils using dual reciprocity methods. Engineering Analysis with Boundary Elements. 2020; 119: 280 - 292.

[46] Srinita SA, Nielsen DR, Kirkham D. Steady flow of water through a two-layer soil. Water Resour. Res. 1969; 5(5): 1053 - 1063.

[47] Srivastava R, Yeh TCJ. Analytical solution for one-dimensional, transient infiltration toward the water table in homogeneous and layered soils. Water Resour. Res. 1991; 27(5): 753 - 762.

[48] van Dam J, Feddes R. Numerical simulation of infiltration, evaporation and shallow groundwater levels with the Richards equation. J. Hydrol. 2000; 233(1): 72 - 85.

[49] Vrugt JA, Hopmans JW, Simunek J. Calibration of a Two-Dimensional Root Water Uptake Model. Soil Sci. Soc. Am. J. 2001; 65: 1027 - 1037.

[50] Warrick AW, Lomen DO. Time-Dependent Linearized Infiltration: III. Strip and Disk Sources. Soil Sci. Soc. Am. J. 1976; 40: 639 - 643.

[51] Waechter RT, Philip JR. Steady two- and three-dimensional flows in unsaturated soil: the scattering analog. Water Resour. Res. 1985; 21(12): 1875 - 1887.

[52] Waechter RT, Mandal AC. Steady Infiltration From a Semicircular Cylindrical Trench and a Hemispherical Pond Into Unsaturated Soil. Water Resour. Res. 1993; 29(2): 457 - 467.

[53] Walter MT, Kim JS, Steenhuis TS, Parlange JY, Heilig A, Braddock RD, Selker JS, Boll J. Funneled flow mechanisms in a sloping layered soil: Laboratory investigation. Water Resour. Res. 2000; 36(4): 841 - 849.

[54] Wever N, Fierz C, Mitterer C, Hirashima H, Lehning M. Solving Richards equation for snow improves snowpack meltwater runoff estimations in detailed multi-layer snowpack model. The Cryosphere. 2014; 8: 257 - 274.

[55] Zhu S, Satravaha P. An efficient computational method for modelling transient heat conduction with nonlinear source terms. Applied Mathematical Modelling. 1996; 20(7): 513 - 522.